21.2 A COMPARISON OF BOUNDARY LAYER WIND PROFILERS FOR USE WITH SPACE LAUNCH VEHICLES

John M. Orcutt*, Robert E. Barbré, Jr., James C. Brenton
Jacobs Space Exploration Group, Huntsville, AL

Patrick White
NASA Marshall Space Flight Center, Huntsville, AL

1. INTRODUCTION

The United States Air Force (USAF) operates two space launch ranges, the Eastern Range (ER) and the Western Range (WR). The ER is primarily located at the Cape Canaveral Air Force Station (CCAFS) and the WR is located at the Vandenberg Air Force Base (VAFB). Multiple systems are used to measure the atmosphere at both ranges, including a suite of 915-MHz Doppler Radar Wind Profilers (DRWP). The 915-MHz DRWPs are used to measure winds in the lowest few kilometers of the atmosphere, primarily in the boundary layer. Boundary layer winds are important during launch, and observations of such can be used as input to toxic dispersion and low-level abort trajectory models. However, these 915-MHz systems are nearing the end of their service life and need to be replaced by systems with similar, or greater, capabilities. The USAF funded evaluations of two systems: a 449-MHz DRWP and a Lidar. Both systems were stationed at each range for separate periods of approximately three months from November 2017 through May 2018. The USAF also funded NASA's Marshall Space Flight Center (MSFC) Natural Environments Branch (NE) to evaluate wind output from the two systems. MSFC NE conducted analysis to demonstrate the system's wind accuracy relative to measurements from the Automated Meteorological Profiling System (AMPS) (Divers et al., 2000), data availability, and Effective Vertical Resolution (EVR).

2. INSTRUMENTATION SYSTEMS

The Lidar and 449-MHz DRWP systems were co-located at the AMPS launch facility at both ranges. For each range, the closest 915-MHz DRWP to the AMPS launch facility was used for the current analysis, with separations of approximately five kilometers.

The 449-MHz system operated in two modes throughout the period. At the ER, the low mode observed wind data from approximately 100 m to approximately 3,000 m above ground level (AGL) in 67-m intervals, and the high mode observed wind data from 1,600 m to 7,000 m AGL in 81-m intervals. Both modes recorded observations every five minutes

At the WR, the low mode observed wind data from 76 m to approximately 3,000 m AGL in 64-m intervals, and the high mode observed wind data from 1,700 m to 7,500 m AGL in 77-m intervals.

The Lidar provided a vertical wind profile approximately every three seconds from 400 m to 3,000 m AGL. The Lidar was co-located with the AMPS launch facility at the ER, and observed data from 2/5/2018 – 4/30/2018. The Lidar was co-located with the AMPS launch facility at the WR from 11/20/2017 – 01/19/2018. It was then sent to the ER for approximately three months before being sent back to the WR where it was placed on top of Tranquillion Peak (elevation of approximately 650 m above mean sea level) from 5/10/2018 – 5/30/2018 to make observations above the marine layer.

The 915-MHz DRWPs measured boundary layer winds from 130 m to 6,000 m AGL in 100-m intervals (Lambert et al., 2003). Although placeholders exist in the output data files for data records up to 6,000 m, typical maximum altitudes were lower. At the WR, there existed six 915-MHz DWPs at fixed locations within the range. This analysis utilized data from the site at Space Launch Complex 2, which is located approximately 5 km from the AMPS facility. At the ER, there existed five 915-MHz DRWPs at fixed locations within the range. This analysis utilized the 915-MHz DRWP at South Cape which is located approximately 5 km away from the AMPS launch facility.

AMPS balloons were released four times a day during the period of record shown in Table 1. Releases of Low Resolution Flight Elements (LR) occurred at 00Z, 06Z, 12Z, and 18Z. Additionally, the AMPS archive included LR balloons released during other times. The LR balloons can reach over 30,000 m and report data in one-second intervals. MSFC NE processed the one-second data for this study. Table 1 provides the period of record for each system and range.

3. ANALYSIS

MSFC NE conducted three analyses to evaluate the 449-MHz DRWP and Lidar. The first analysis compared westerly (U) and southerly (V) wind component profiles to concurrent AMPS measurements to quantify the difference of both systems relative to AMPS observations. Data from the AMPS system was used as the standard measurement for comparisons as it provides direct measurements of the atmosphere. The second analysis consisted of assessing data availability

**Corresponding author address:* John M. Orcutt., Jacobs Space Exploration Group, 620 Discovery Dr., Huntsville, AL 35806; email: john.m.orcutt@nasa.gov.

versus altitude, which quantifies how often one should expect to obtain data to an altitude of interest.

Table 1: Period of record for data from both ER and WR

Range	System	Period of Record
ER	AMPS	1/16/18 – 4/27/18
ER	449-MHz DRWP	1/22/18 – 4/27/18
ER	Lidar	2/5/18 – 4/30/18
ER	915-MHz DRWP	2/1/18 – 4/29/18
WR	AMPS	11/20/17 – 3/14/18, 5/10/18 – 5/30/18
WR	449-MHz DRWP	12/1/17 – 3/4/18
WR	Lidar	11/20/17 – 1/29/18, 5/10/18 – 5/30/18
WR	915-MHz DRWP	11/20/17 – 3/14/18

The third analysis comprised of examining the EVR of each system, which quantifies the wavelengths of the wind features that each system resolves. MSFC NE additionally evaluated wind profiles from the existing 915-MHz DRWPs in the vicinity of the 449-MHz DRWP and Lidar at each range for reference.

3.1 *Comparison Of Wind Profiles To Concurrent Balloon Observations*

MSFC NE compared wind component profiles from the 449-MHz DRWP, 915-MHz DRWP, and Lidar to concurrent wind component profiles from the AMPS system. Data from each remote sensing system were temporally and vertically matched to AMPS data to account for differences in measurement characteristics between the given system and AMPS. Table 2 provides a summary of the parameters used to temporally and vertically match profiles.

AMPS profiles were vertically matched to the 449-MHz DRWP by block averaging the AMPS data in 65-m or 77-m intervals, depending on which mode was being examined, centered on the 449-MHz DRWP altitude. The AMPS data were temporally matched to the 449-MHz data by finding a concurrent 449-MHz DRWP profile that existed within ± 2.5 minutes from the AMPS observation at a specified altitude. Then the vertically averaged AMPS profile and the temporally matched 449-MHz DRWP profile were used to calculate the difference in the wind components (ΔU and ΔV, respectively). This procedure was performed for both ranges for observations with a corresponding quality control (QC) flag of at least 0.8, as it was understood that operational meteorologists use this value as a data quality check (Tim Wilfong, personal communication).

The 915-MHz DRWP was compared to AMPS data using concurrent 915-MHz DRWP profiles that were vertically matched. AMPS profiles were vertically matched to the 915-MHz DRWP profiles by block averaging the AMPS data in 101-m intervals. In order to be compared to an AMPS measurement, the 915-MHz DRWP profile had to exist within ±7.5 minutes of the first AMPS observation. This procedure was performed at both ranges without implementing any QC.

The Lidar wind profiles were compared to AMPS wind profiles using concurrent observations existing within ±2.5 seconds of each AMPS data timestamp at measurement altitudes that existed within ±9 m of the Lidar altitude. No block averaging was performed on the AMPS data for the Lidar analysis due to the fine temporal sampling of the Lidar. This procedure was performed at both ranges using previously-QC'ed data.

MSFC NE computed the sample size, mean wind component deltas, root-mean-square (RMS) wind component deltas, and 99% envelopes of the wind component deltas versus altitude for all systems to characterize the deltas relative to AMPS measurements. It is important to note that deltas from concurrent AMPS measurements do not equate to the absolute error of the system for two primary reasons. First, AMPS observations contain their own measurement error. Second, valid measurements from multiple systems sampling different wind regimes (which is driven by balloons drifting with the wind) contribute to the calculated delta between concurrent reports from said systems. Computations of the mean, RMS, and 99% envelope were retained at a given altitude if at least 10, 30, and 100 comparisons, respectively, existed at that altitude.

3.2 *Data Availability*

An analysis of data availability versus altitude was conducted for all systems. The objective of this analysis entails showing the probability of receiving vertically complete profiles, from a given system, within a specified altitude range. For a given system, the number of profiles that contained data at all altitudes between the bottom of the profile and each subsequent altitude was tallied. The data availability was then computed as the quotient of this quantity and the number of profiles that existed.

Table 2: For each remote sensing system, the vertical averaging interval applied to balloon profiles, and the criteria defining a concurrent record relative to AMPS data.

System	Vertical Averaging Interval	Temporal Criteria
449-MHz DRWP, Low	67 m (ER), 64 m (WR)	+/- 2.5 minutes
449-MHz DRWP, High	81 m (ER), 77 m (WR)	+/- 2.5 minutes
915-MHz DRWP	101 m	+/- 7.5 minutes
Lidar	9 m (no averaging)	+/-2.5 seconds

3.3 *Effective Vertical Resolution*

Analysis of mean Power Spectral Density (PSD) and magnitude-squared coherence (referred to as "coherence" herein) were conducted to estimate the EVR of each system. The methodology used followed

Merceret (1999), who calculated the composite-mean PSD and coherence of wind component profiles from daily averaged quantities. For an individual day, wind component profile pairs spaced by a specified time were extracted. Both profiles within the pair had to contain continuous data within specified altitude ranges. Table 3 shows the temporal spacing between pairs, the required altitude ranges, and vertical sampling interval for each system. The vertical sampling interval equates to half of the smallest wavelength of vertical features that the system is capable of resolving. The time between pairs corresponds to the temporal sampling capabilities of each system. Once the profiles and pairs were determined, the linear trend was removed from each wind component profile and a Hanning window with zero overlap was applied to the profile. Next, the Fast Fourier Transform (FFT) of each profile was computed as a function of wavelength and used to generate each profile's PSD and each pair's Cross-Spectral Density (CSD). These quantities were then used to compute the coherence. Coherence describes the relationship between two signals at each wavelength, where incoherent noise dominates this relationship at values below 0.25, as this value corresponds to a signal-to-noise ratio of unity. The coherence is given as:

$$Coh^2 = \frac{|\langle CSD \rangle|^2}{\langle PSD_1 \rangle \langle PSD_2 \rangle} \qquad (1)$$

where brackets denote averages over the entire day at each wavelength. Averaging must be performed in order to avoid the coherence resulting in unity. The mean coherence was calculated for each day following Eq. (1). Last, the composite PSD and coherence were generated by computing a sample-size-weighted PSD and coherence at each wavelength from the daily mean quantities. For reference, Wilfong (2017) found the EVR of AMPS one-second LR profiles to be and 270 m.

Table 3: Attributes of data used for the EVR analysis from each system

System	Time Between Pairs (s)	Required Altitudes (m AGL)	Sampling Interval (m)
449-MHz DRWP Low Mode	300	102 – 2,065 (ER) 76 – 2,007 (WR)	67.7 (ER) 64.0 (WR)
449-MHz DRWP High Mode	300	1,742 – 3,038 (ER) 1,636 – 3,022 (WR)	81.0 (ER) 77.0 (WR)
Lidar	1-15 seconds	400 – 2,500 (ER and WR)	100.0 (ER and WR)

4.0 RESULTS

4.1 *Balloon Comparison – ER*

Up to 305 concurrent AMPS reports were used to compute statistical quantities of wind component deltas at the ER. Sample size versus altitude varied because the remote sensing systems did not contain data at all altitudes. Typically, the number of reports decreased with altitude due to weaker return signal. Figure 1 shows the number of samples used in the AMPS comparison for the ER. The sample size peaked around 1,000 m. The 449-MHz DRWP had the greatest number of samples for comparison at approximately 500 m, and then the sample size gradually decreased with altitude up to approximately 7,500 m. The lower sample size of the Lidar comparisons attributed to numerous cases when the Lidar did not report a wind at the timestamp and altitude of the AMPS data. The 915-MHz DRWP sample size was comparable to the sample size of the Lidar, especially from approximately 1,000 – 2,000 m. Table 4 presents the altitude ranges over which statistical quantities from each system were computed for the ER.

Table 4: Altitude range (AGL) over which the mean, RMS, and 99% envelope were computed from each system at the ER.

System	Mean (m AGL)	RMS (m ALG)	99% Envelope (m AGL)
915-MHz DRWP	130 – 4,683	130 – 4,380	130 – 2,660
449-MHz DRWP Low Mode	102 – 3,148	102 – 3,148	169 – 3,148
449-MHz DRWP High Mode	1,742 – 7,493	1,742 m – 7,007	1,742 – 5,387
Lidar	400 – 3,000	400 – 3,000	400 – 3,000

Figure 1: Number of comparisons to concurrent AMPS data versus altitude (AGL) for the 449-MHz DRWP, Lidar, and 915-MHz DRWP at the ER.

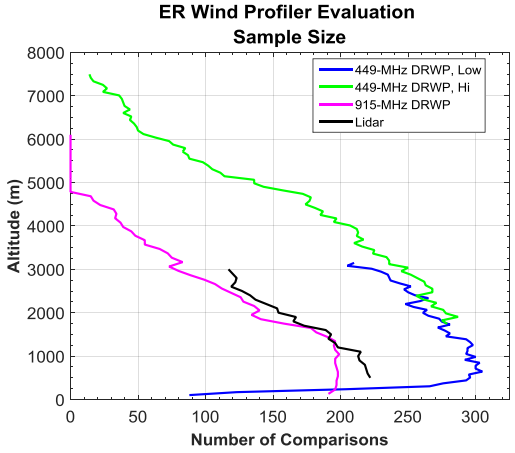

Figures 2 and 3 display the mean ΔU and ΔV, respectively, as a function of altitude. The Lidar and 449-MHz DRWP low mode reported mean deltas within 0.5 m/s of concurrent AMPS winds, with a slight positive bias noted in ΔU from both systems and in ΔV from the 449-MHz DRWP. A slight negative bias was noted in ΔV from the Lidar. The 449-MHz DRWP high mode comparison showed mean deltas ranging from approximately -0.5 m/s to 1.1 m/s, with a slight positive bias noted. The 915-MHz DRWP comparison showed mean deltas within 0.5 m/s of concurrent AMPS winds up to approximately 2,000 m altitude. Above this altitude, deltas between AMPS and 915-MHz DRWP output show a positive bias, with the mean ΔU increasing to approximately 1.0 m/s and mean ΔV increasing to approximately 2.2 m/s.

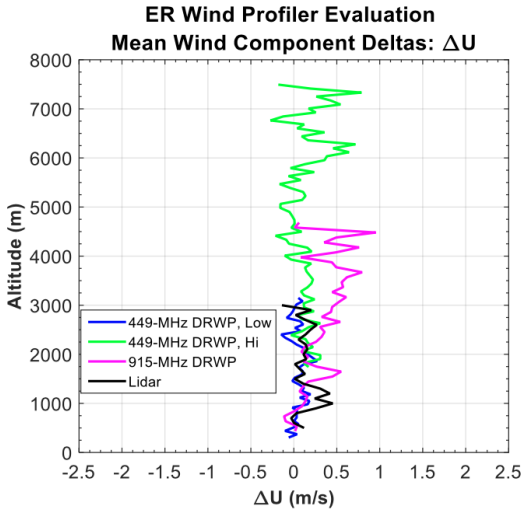

Figure 2: Mean ΔU versus altitude (AGL) between concurrent data from the 449-MHz DRWP, 915-MHz DRWP and Lidar with AMPS data at the ER.

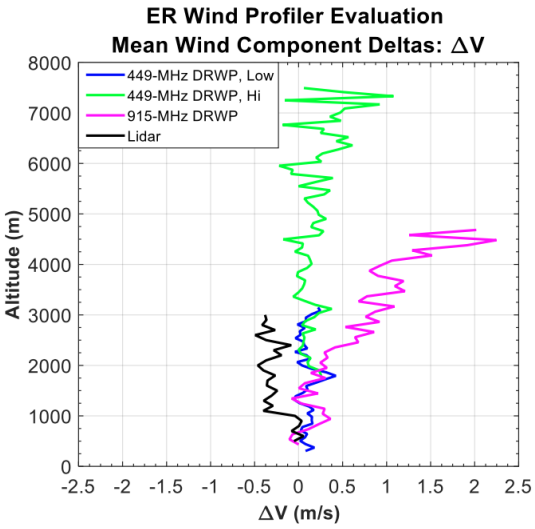

Figure 3: Mean ΔV versus altitude (AGL) between concurrent data from the 449-MHz DRWP, 915-MHz DRWP, and Lidar data at the ER.

The RMS wind component deltas, shown in Figures 4 and 5, provided an estimate of the error of each system (relative to AMPS measurements), including the system's bias. With the exception of the 449-MHz DRWP at the lowest altitudes, the 449-MHz DRWP low mode and Lidar both reported RMS deltas of approximately 1.1 – 1.7 m/s at a given altitude. The 449-MHz high mode showed RMS deltas of approximately 1.2 – 2.1 m/s at a given altitude, with more variation in this quantity existing across its altitude range relative to the 449-MHz DRWP low mode and Lidar results.

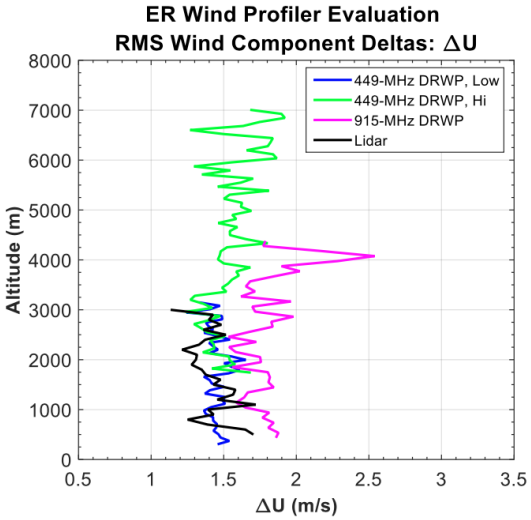

Figure 4: RMS of the ΔU versus altitude (AGL) between concurrent data from the 449-MHz DRWP, 915-MHz DRWP, and Lidar with AMPS data at the ER.

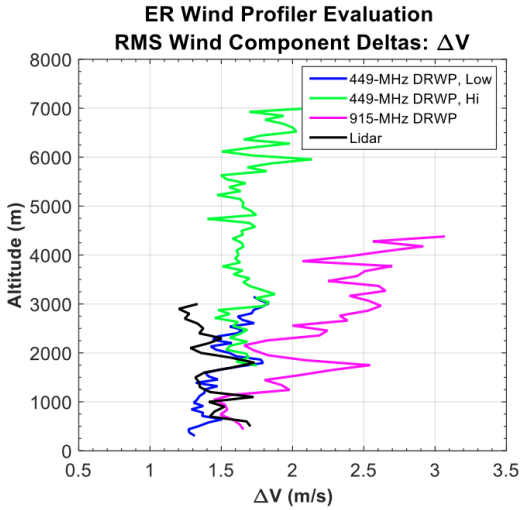

Figure 5: RMS of ΔV versus altitude (AGL) between concurrent data from the 449-MHz DRWP, 915-MHz DRWP, and Lidar with AMPS data at the ER.

The 915-MHz DRWP showed larger RMS deltas, with the RMS ΔU between roughly 1.5 – 2.0 m/s at the majority of altitudes. The RMS ΔV from the 915-MHz DRWP increased readily with increasing altitude and ranged from approximately 1.5 m/s at 1,000 m to approximately 3.0 m/s at 4,500 m.

The 99% envelope of the wind component deltas (i.e., the wind component deltas at the 0.05% and 99.5% probability level) at each altitude, shown in Figure 6 and 7, characterizes extreme deltas from each system. These deltas approximate ± 5 m/s at many altitudes, with a couple of outliers noted that approach ± 10 m/s.

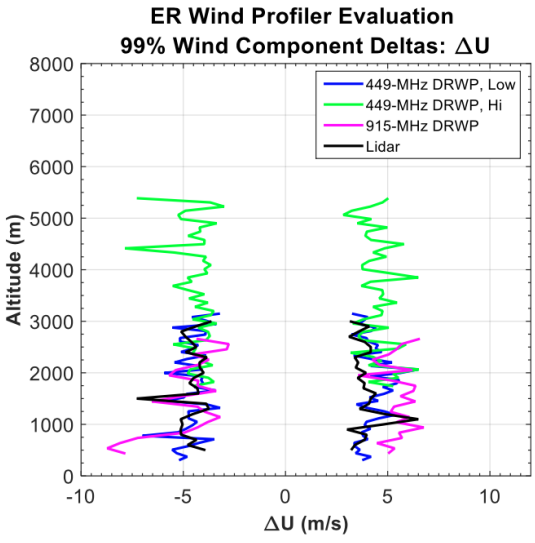

Figure 6: 99% envelope of ΔU versus altitude (AGL) between concurrent data from the 449-MHz DRWP, 915-MHz DRWP, and Lidar with AMPS data at the ER.

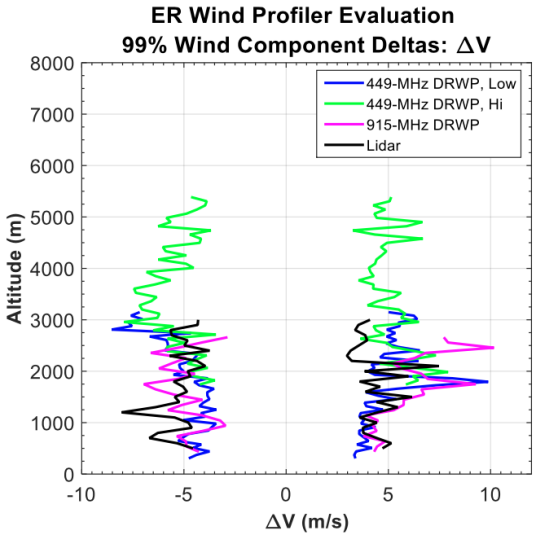

Figure 7: 99% envelope of ΔV versus altitude (AGL) between concurrent data from the 449-MHz DRWP, 915-DRWP, and Lidar with AMPS data at the ER.

4.2 *Balloon Comparison – WR*

Figure 8 shows the number of comparisons used in the AMPS comparison for the WR. Sample size peaked at the lowest altitudes of each respective system. As with the ER, the lower sample size of the Lidar comparisons resulted in numerous cases when the Lidar did not report a wind at the timestamp and altitude of the AMPS data. Below approximately 1,000 m, the Lidar contained the fewest number of samples at a given altitude, followed by the 915-MHz DRWP, and then the 449-MHz DRWP. The 915-MHz DRWP contains the fewest comparisons above 1,000 m.

Table 5 presents the altitude ranges over which statistical quantities from each system were computed for the WR. Note that statistical quantities of comparisons between the Lidar and AMPS wind components were not generated for the period when the Lidar operated at Tranquillion Peak. This attribute occurred because too few samples existed to compute any of the statistical quantities (Figure 8, dashed-line). All Lidar results presented in Table 5 and Figures 9 – 12 stem from the collection period when the Lidar was co-located with the other systems, and not on Tranquillion Peak.

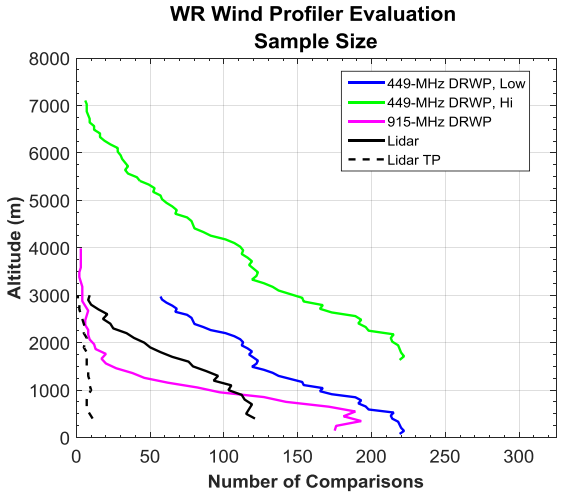

Figure 8: Number of comparisons to concurrent AMPS data versus altitude (AGL) for the 449-MHz DRWP, Lidar, and 915-MHz DRWP at the WR.

Table 5: Altitude range (AGL) over which the mean, RMS, and 99% envelope were computed from each system at the WR.

System	Mean (m AGL)	RMS (m AGL)	99% Envelope (m AGL)
915-MHz DRWP	145 – 1,966	145 – 1,359	145 – 853
449-MHz DRWP Low Mode	76 – 2,973	76 – 2,973	76 – 2,201
449-MHz DRWP High Mode	1,636 – 6,565	1,636 – 5,949	1636 – 4,177
Lidar	400 – 2,800	400 – 2,200	400 – 1,100

Figure 9 and 10 display the mean wind component deltas as a function of altitude. The Lidar and 449-MHz DRWP Low mode reported mean deltas within 0.5 m/s of concurrent AMPS winds, with a slight positive bias noted in ΔU from the Lidar and a slight negative bias noted in ΔU from the 449-MHz DRWP. The 449-MHz high mode comparison showed a slight positive bias ΔU at some altitudes and a slight negative bias in ΔV at all altitudes. The 915-MHz DRWP reported mean wind component deltas ranging from approximately -1.0 m/s to 1.0 m/s at the majority of altitudes. Also, more variation in the mean wind component deltas are noted from the 915-MHz DRWP relative to the other systems at the applicable altitudes (i.e., below 2,000 m).

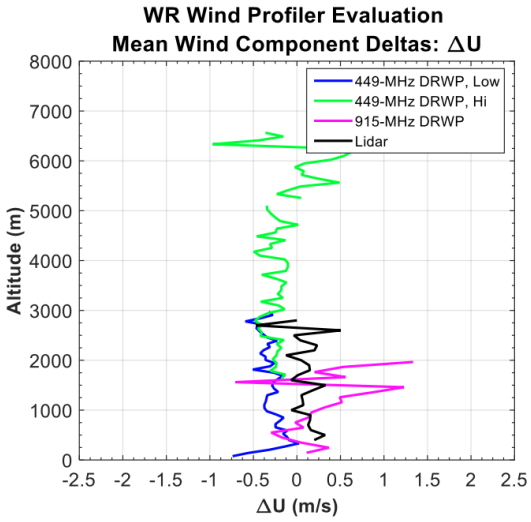

Figure 9: Mean ΔU versus altitude (AGL) between concurrent data from the 449-MHz DRWP, 915-MHz DRWP, and Lidar with AMPS data at the WR.

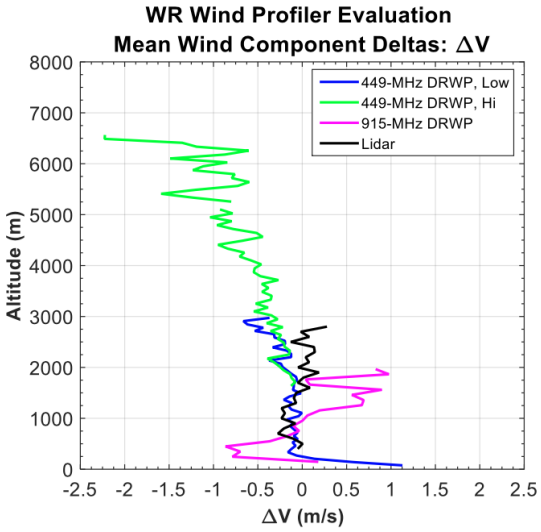

Figure 10: Mean ΔV versus altitude (AGL) between concurrent data from the 449-MHz DRWP, 915-MHz DRWP, and Lidar with AMPS data at the WR.

The RMS wind component deltas, shown in Figure 11 and 12, provided an estimate of the error of each system (relative to AMPS measurements), including the system's bias. With the exception of the 449-MHz DRWP at the lowest altitudes and the outlier at 5,179 m, the 449-MHz DRWP (low and high modes) and Lidar both reported RMS deltas of roughly 1.5 – 2.0 m/s at a given altitude. The Lidar produced slightly lower RMS deltas than the 449-MHz DRWP at each altitude. The 915-MHz DRWP produced RMS deltas ranging from approximately 1.5 – 2.5 m/s at a given altitude, and exceeded the RMS deltas from the 449-MHz DRWP and Lidar at the majority of altitudes.

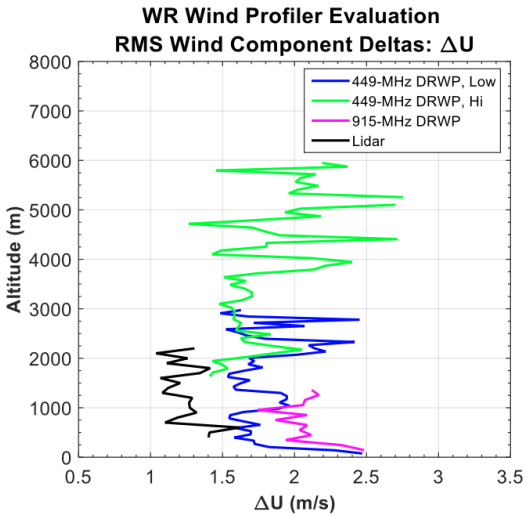

Figure 11: RMS of the ΔU versus altitude (AGL) between concurrent data from the 449-MHz DRWP, 915-MHz DRWP, and Lidar with AMPS data at the WR.

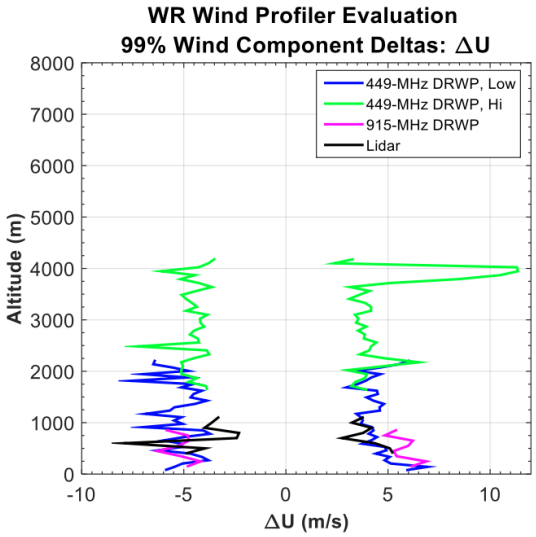

Figure 13: 99% envelope of ΔU versus altitude (AGL) between concurrent data from the 449-MHz DRWP, 915-MHz DRWP, and Lidar with AMPS data at the WR.

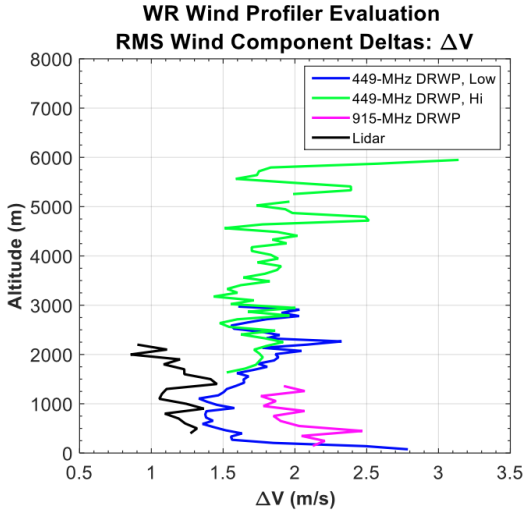

Figure 12: RMS of ΔV versus altitude (AGL) between concurrent data from the 449-MHz DRWP, 915-MHz DRWP, and Lidar with AMPS data at the WR.

The 99% envelope of the wind component deltas (i.e., the wind component deltas at the 0.05% and 99.5% probability level) at each altitude, shown in Figures 13 and 14, characterized extreme wind component deltas from each system. These deltas approximated ± 5 m/s at many altitudes, with deltas at a couple of altitudes (most notably ΔU from the 449-MHz DRWP near 4,000 m) that were near ± 10 m/s.

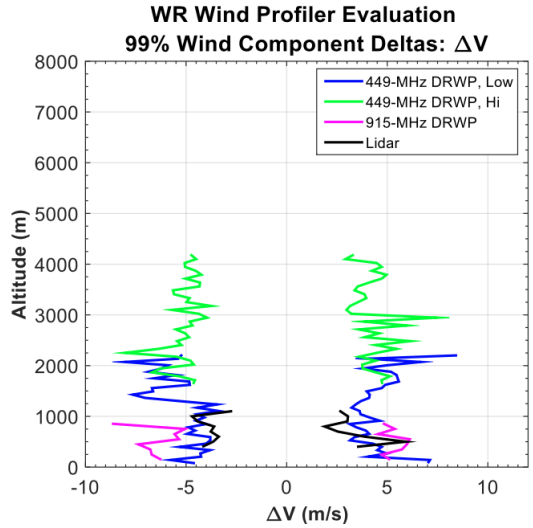

Figure 14: 99% envelope of ΔV versus altitude (AGL) between concurrent data from the 449-MHz DRWP, 915-MHz DRWP, and Lidar with AMPS data at the WR.

4.3 *Data Availability – ER*

Figure 15 shows the percent data availability for all systems at the ER. Availability at the lowest altitudes were at or near 100%, and then the number of available profiles decreased with increasing altitude. One should interpret this figure as the number of complete profiles from the lowest altitude AGL of the system to the altitude specified on the ordinate, given that a profile existed. The data availability for the 915-MHz DRWP and Lidar decreased at nearly the same rate up to 3,000 m, which

is the highest altitude recorded from the Lidar data utilized in this study. The 449-MHz DRWP low mode had greater data availability than both the 915-MHz DRWP and Lidar above approximately 1,000 m.

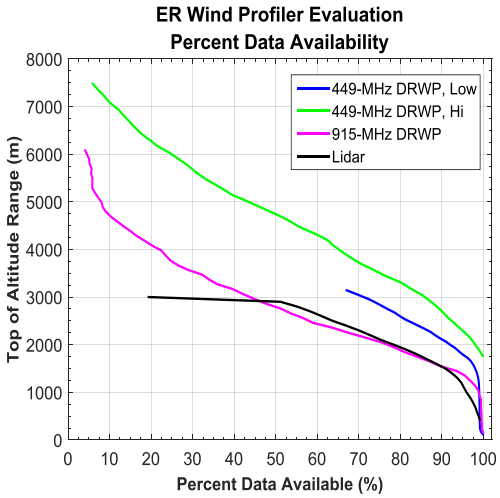

Figure 15: Percent of data available between the lowest altitude of the system and the selected altitude on the ordinate for all systems at the ER.

4.4 *Data Availability – WR*

Figure 16 shows the percent data availability for all systems at the WR. As with the ER, availability at the lowest altitudes were at or near 100%, and then the number of available profiles decreased with increasing altitude range. The data availability for the 915-MHz DRWP decreased the most rapidly with increasing altitude. Up to approximately 700 m, the 915-MHz DRWP data availability decreased at near the same rate as the Lidar availability. From approximately 700 – 3,000 m, the 915-MHz DRWP availability decreased more rapidly than the other systems.

WR Lidar data availability was examined separately for the data collection periods before and during the system's placement on Tranquillion Peak. During the former period, 90% of the profiles extended to 1,000 m, but only 40% of the profiles reached 2,000 m. During the latter period, 80% of the profiles reached 1,000 m, but 60% of the profiles reach 2,000 m. Thus, during the latter period relative to the former period, fewer profiles reached 1,000 m; but profiles that did reach 1,000 m were more likely to reach 2,000 m. Data availability from both systems decreased at a similar rate for altitudes between 2,000 m and 3,000 m.

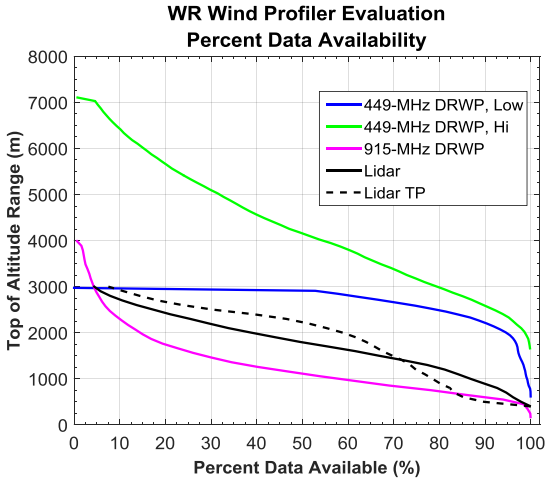

Figure 16: Percent of data available between the lowest altitude of the system and the selected altitude on the ordinate for all systems at the WR.

4.5 *Effective Vertical Resolution – ER*

Figures 17 and 18 present the EVR analysis results for the Lidar and 449-MHz DRWP at the ER. Each system's coherence remained above 0.25 at all wavelengths, which indicates that the EVR of the system is limited to its Nyquist wavelength, which is two times the vertical sampling interval of the instrument. The EVR of the Lidar, 449-MHz DRWP low mode, and 449-MHz DRWP high mode is 200 m, 134 m, and 162 m, respectively.

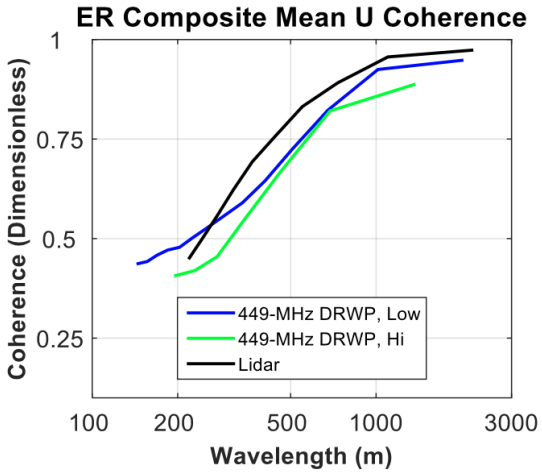

Figure 17: Composite mean U coherence for the ER systems.

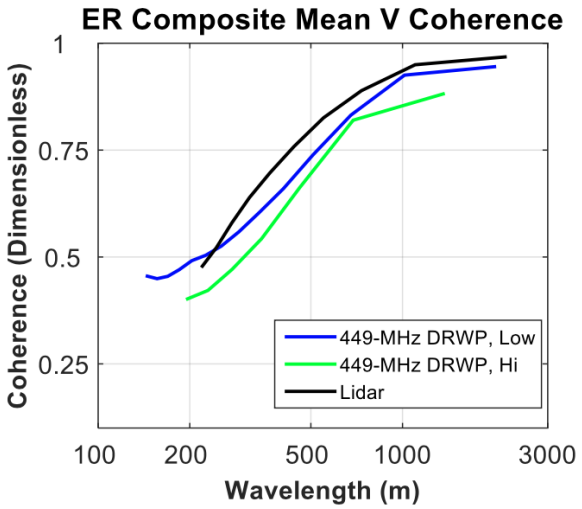

Figure 18: Composite mean V coherence for the ER systems.

4.6 *Effective Vertical Resolution – WR*

Figures 19 and 20 present the EVR analysis results for the Lidar and 449-MHz DRWP at the WR. Each system's coherence remained above 0.25 at all wavelengths, which indicates that the EVR of the system is limited to its Nyquist wavelength, which is two times the vertical sampling interval of the instrument. The EVR of the Lidar, 449-MHz DRWP low mode, and 449-MHz DRWP high mode is 200 m, 128 m, and 154 m, respectively.

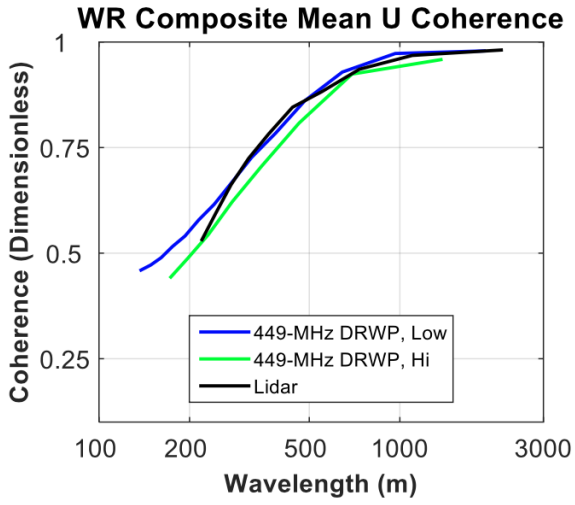

Figure 19: Composite mean U coherence for the WR systems.

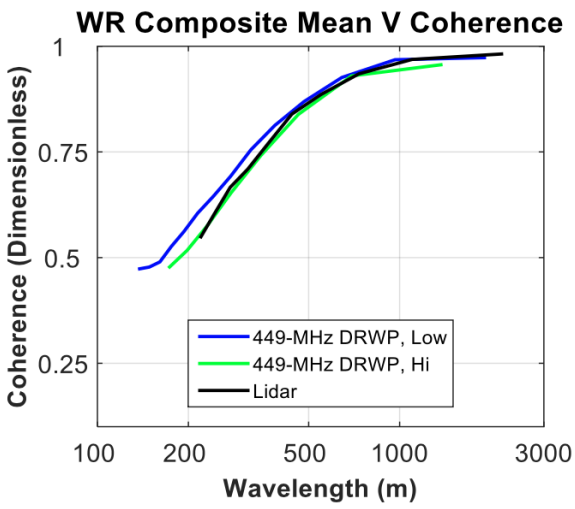

Figure 20: Composite mean V coherence for the WR systems.

5. SUMMARY

This report documents analyses conducted to evaluate wind profile output from the 449-MHz DRWP and Lidar systems, which took measurements at the ER and WR from November 2017 through May 2018. Analyses comprised of comparing wind components from the systems to concurrent AMPS wind profiles, examining the percent of complete profiles that reached specified altitudes from the bottom of the profile, and quantifying each system's EVR.

While some exceptions existed, the mean, RMS, and 99% delta of each system was approximately 1.0 m/s, 1.5 – 2.0 m/s, and 5.0 m/s at a given altitude, respectively. Slightly higher mean and RMS deltas were noted from the 449-MHz DRWP at the lowest few altitudes (at both ranges), and from the 449-MHz DRWP at the higher altitudes at the WR. The Lidar produced a slightly greater negative bias in ΔV at the ER. Results for wind comparisons and EVR compare well with previously documented studies of AMPS measurements.

The percent of available profiles from all systems decreased or remained constant with increasing altitude. The 449-MHz DRWP tended to have higher data availability than the Lidar, and the high-mode recorded data up to 7,000 – 8,000 m. The Lidar showed different characteristics at the WR before and after its placement on Tranquillion Peak. During the latter period relative to the former period, fewer profiles reached 1,000 m; but profiles that did reach 1,000 m were more likely to reach 2,000 m.

All systems evaluated in this study were found to be Nyquist-limited. As such, the 449-MHz DRWP low mode, 449-MHz DRWP high mode, and Lidar were found to resolve vertical wind features with wavelengths as small as 128 m, 154 m, and 200 m, respectively. One should

note that the DRWP and Lidar systems produce wind profiles much more frequently than AMPS releases, but tend to have a smaller vertical coverage and a coarser sampling interval.

6. ACKNOWLEDGEMENTS

Much appreciation goes to numerous personnel at multiple organizations who helped with this project. RGNext supplied the data from all Lidar and DRWP systems at both ranges. Neil Cantwell / RGNext served as the Technical Point of Contact during this study, and graciously addressed several questions about the data. Many thanks go to the reviewers of this report. This work was performed under contract 80MSFC18C0011.

7. REFERENCES

Divers, Bob, P. Viens, T. Mitchell, K. Bzdusek, G. Herman and R. Hoover, 2000: Automated Meteorological Profiling System (AMPS) Description. *Proc. Ninth Conf. on the Aviation, Range and Aerospace Meteorology,* Dallas, TX. Amer. Meteor. Soc.

Lambert, W. C., F. J. Merceret, G. E. Taylor, and J. G. Ward, 2003: Performance of Five 915-MHz Wind Profilers and an Associated Automated Quality Control Algorithm in an Operational Environment. *J. Atmos. Oceanic Technol.,* 20, 1488–1495.

Merceret, F., 1999: The Vertical Resolution of the Kennedy Space Center 50 MHz Wind Profiler, *Jounal of Atmospheric and Oceanic Technology,* vol. 16, pp. 1273-1278.

Wilfong, T. 2012: AMPS II Eastern Range Formal DT&E Analysis, Boulder, CO.